Crystal structure of the C2 domain from protein kinase C-δ

H Pappa[1], J Murray-Rust[1], LV Dekker[2†], PJ Parker[2] and NQ McDonald[1,3*]

Background: The protein kinase C (PKC) family of lipid-dependent serine/threonine kinases plays a central role in many intracellular eukaryotic signalling events. Members of the novel (δ, ε, η, θ) subclass of PKC isotypes lack the Ca^{2+} dependence of the conventional PKC isotypes and have an N-terminal C2 domain, originally defined as V0 (variable domain zero). Biochemical data suggest that this domain serves to translocate novel PKC family members to the plasma membrane and may influence binding of PKC activators.

Results: The crystal structure of PKC-δ C2 domain indicates an unusual variant of the C2 fold. Structural elements unique to this C2 domain include a helix and a protruding β hairpin which may contribute basic sequences to a membrane-interaction site. The invariant C2 motif, Pro–X–Trp, where X is any amino acid, forms a short crossover loop, departing radically from its conformation in other C2 structures, and contains a tyrosine phosphorylation site unique to PKC-δ. This loop and two others adopt quite different conformations from the equivalent Ca^{2+}-binding loops of phospholipase C-δ and synaptotagmin I, and lack sequences necessary for Ca^{2+} coordination.

Conclusions: The N-terminal sequence of Ca^{2+}-independent novel PKCs defines a divergent example of a C2 structure similar to that of phospholipase Cδ. The Ca^{2+}-independent regulation of novel PKCs is explained by major structural and sequence differences resulting in three non-functional Ca^{2+}-binding loops. The observed structural variation and position of a tyrosine-phosphorylation site suggest the existence of distinct subclasses of C2-like domains which may have evolved distinct functional roles and mechanisms to interact with lipid membranes.

Addresses: [1]Structural Biology and [2]Protein Phosphorylation Laboratories, Imperial Cancer Research Fund, 44 Lincoln's Inn Fields, London WC2A 3PX, UK and [3]Department of Crystallography, Birkbeck College, London WC1E 7HX, UK.

[†]Present address: Department of Medicine, The Rayne Institute, 5 University Street, London WC1E 6JJ, UK.

*Corresponding author.
E-mail: mcdonald@icrf.icnet.uk

Key words: calcium, crystal structure, C2 domain, protein kinase C, superfamily

Received: **6 April 1998**
Revisions requested: **6 May 1998**
Revisions received: **21 May 1998**
Accepted: **28 May 1998**

Structure 15 July 1998, **6**:885–894
http://biomednet.com/elecref/0969212600600885

Introduction

The protein kinase C (PKC) family of lipid-activated serine/threonine kinases comprise a diverse family of isozymes that can be classified according to their domain structure and cofactor requirements [1,2]. The main classes of PKC molecules are the conventional (also known as classical), the novel, the atypical and the μ-like PKCs. The conventional PKCs (α, βI, βII, γ) are activated by both Ca^{2+}-dependent phospholipid binding and diacylglycerol (DAG), while the novel PKCs (δ, ε, η, θ) and μ-like PKCs are activated by DAG and phospholipids in a Ca^{2+}-independent manner. The atypical PKCs (ζ, ι/λ) are not activated by either Ca^{2+} or DAG. Common to all PKC isotypes is a conserved protein kinase domain (C3 and C4 sequences) homologous to the cyclic AMP (cAMP)-dependent protein kinase (cAPK; Figure 1) [3,4]. The more variable N-terminal sequences contain the conserved C1 and C2 modules in addition to a pseudosubstrate sequence that masks protein kinase activity in the absence of PKC activators [5–7]. The position of the C2 module and pseudosubstrate sequence relative to C1 varies between the conventional and novel PKC subclasses (Figure 1).

The C1 and C2 domains are responsible for interaction with PKC activators [7]. DAG and its phorbol-ester analogues bind to the C1 domain [8], while phosphatidylserine and Ca^{2+}, in the case of conventional PKCs, bind to the C2 domain [9,10]. The Ca^{2+}-independent novel PKCs have C2 domains which apparently lack the acidic sidechains required for Ca^{2+} coordination and may bind phosphatidylserine constitutively [6,11]. Interaction of the novel PKC C2 domain with phospholipid influences the binding of phorbol esters to the C1 domain, indicating that both the domains and their respective lipid-binding sites are in close proximity [12]. Other functional roles have been proposed for the novel PKC C2 domain, such as translocating PKC to the plasma membrane through interaction with growth associated protein 43 (GAP43) [13] or to other subcellular compartments through interaction with receptors of activated protein kinase C (RACKs) [14].

The PKC C2 domain belongs to a superfamily of related C2 modules found within numerous proteins involved in membrane trafficking and signal transduction [15]. Crystal structures of C2 domains from synaptotagmin I (SynI), phospholipase C-δ (PLC-δ) and phospholipase A2 (cPLA2) indicate a highly homologous β-sandwich tertiary fold with two topologically distinct circularly permuted variants known as S- and P-type [16–18]. An S-type variant found in the C2A domain of SynI [16] has its Ca^{2+}-binding

Figure 1

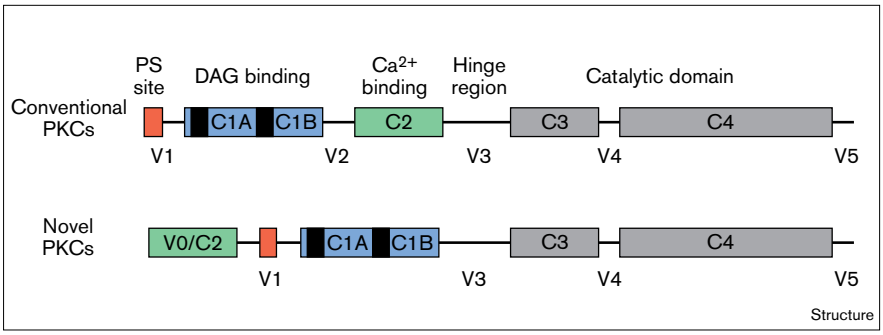

Domain structures of the conventional and novel PKC isotypes. The conserved (C) and variable (V) regions are shown. The C1 region (blue) contains two copies of a zinc-binding cysteine-rich motif, termed C1A and C1B, and is responsible for PKC activation by DAG. The C2 domain (green) is responsible for the Ca^{2+}-dependent binding of phospholipids. The C3 and C4 regions (grey) comprise the catalytic domain and ATP- and substrate-binding sites. The pseudosubstrate sequence (PS) is shown in red and the novel PKC V0/C2 domain in green.

region at the same position as the P-type variant present in PLC-δ [17] and cPLA2 [18]. These studies have revealed the structural basis for Ca^{2+} binding to C2 domains [16–18]. Acidic residues from two Ca^{2+}-binding loops, CBR1 and CBR3, supported by the CBR2 loop, coordinate multiple Ca^{2+} ions. Nuclear magnetic resonance (NMR) studies on the PKC-β C2 domain have confirmed the multivalent nature of the Ca^{2+}-binding site [10]. Although no PKC C2 structures have been published, sequence analysis suggests that the C2 domains of conventional PKCs adopt the topology of an S-type while those of the novel PKCs form a P-type topology [19].

In this paper, we report the crystal structure of a C2 domain from a novel PKC isotype, allowing a detailed structural comparison to be made with other known C2 structures. Several functionally important differences are described that explain the absence of a Ca^{2+}-binding site and the basis for selective tyrosine phosphorylation of PKC-δ [20].

Results and discussion

Structure determination

The C2 domain of rat PKC-δ, comprising residues 1–123, was produced using a bacterial expression system and crystallised as described previously [21]. The highly ordered crystals belong to space group $P2_12_12_1$ with unit cell parameters a, 40.7 Å, b, 60.7 Å, c, 120.9 Å, and have two molecules in the asymmetric unit. The structure was solved using experimental phases derived from selenomethionine and two mercury derivatives. Density modification and two-fold averaging gave an interpretable electron density map that allowed tracing of both copies of the C2 domain in the asymmetric unit. Chain tracing was assisted by assigning density to each of the 10 selenium positions within the asymmetric unit (Figure 2). Refinement with the programs REFMAC and X-PLOR gave a final model with an R factor of 19.5% and a free R factor of 24.5%, using all data between 20.0 Å and 2.2 Å. The root mean square deviation (rmsd) between the two molecules was 0.79 Å for all 123 Cα atoms, indicating the relative flexibility of the molecule.

Overall structure

The crystal structure of the PKC-δ C2 domain confirms that the novel PKC isotypes (δ, ε, η, θ) have an antiparallel β-sandwich structure with a P-type topology similar to that of PLC-δ C2 (Figures 3 and 4). The two β sheets are composed of strands β1, β4, β7, β8 and strands β2, β5, β6, respectively, using the labelling convention of PLC-δ (Figure 5a) [17]. An irregular strand we define as e3 (Figures 3 and 4) replaces strand β3 of the P-type C2 domain (equivalent to β4 of the S-type). Superposition with the C2 domains from SynI and PLC-δ indicates a structurally similar core with an overall rmsd of 1.3 Å for

Figure 2

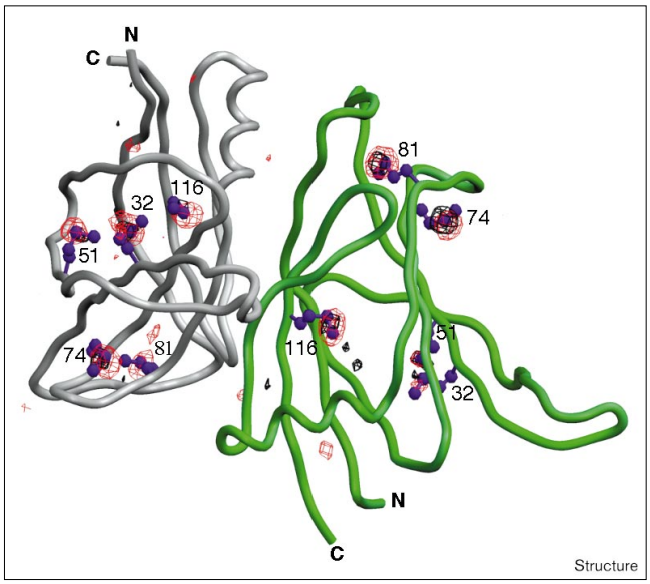

Isomorphous and anomalous difference Fourier maps using selenomethionine data, superimposed on a backbone representation of the two molecules within the asymmetric unit. Experimental phases from the two mercury derivatives were used in map calculation; both maps are contoured at 5σ. The ten selenium sites in the asymmetric unit are labelled according to the methionine residue number. (The figure was produced using the program SETOR [40].)

Figure 3

Two orthogonal views of the fold of PKC-δ C2. Secondary structure elements are sequentially labelled; β strands are shown in green and the single helix in yellow. (The figure was prepared using the program SETOR [40].)

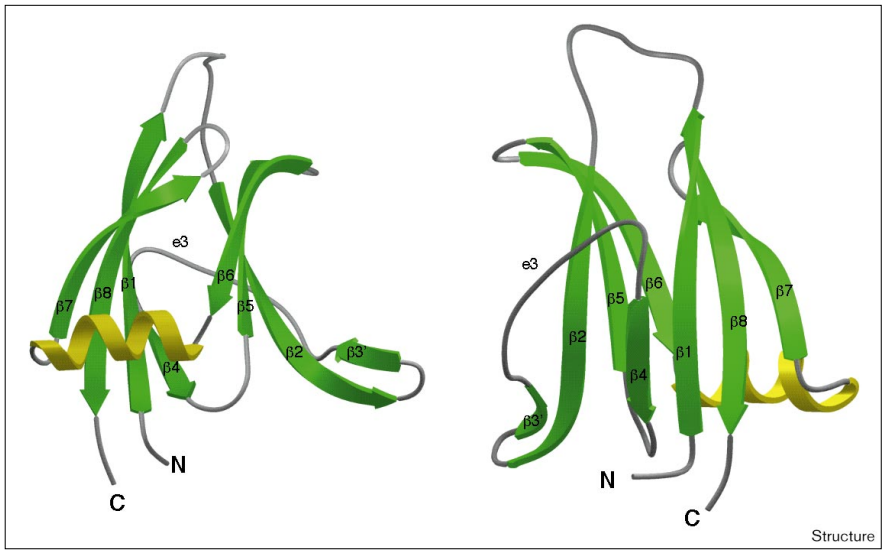

69 Cα atoms from PLC-δ C2 and 1.7 Å for 85 Cα atoms from SynI C2A (Figure 6). This is comparable to an rmsd of 1.4 Å for 109 equivalent α carbons between the PLC-δ and SynI C2s reported by Essen *et al.* [17]. Structural

Figure 4

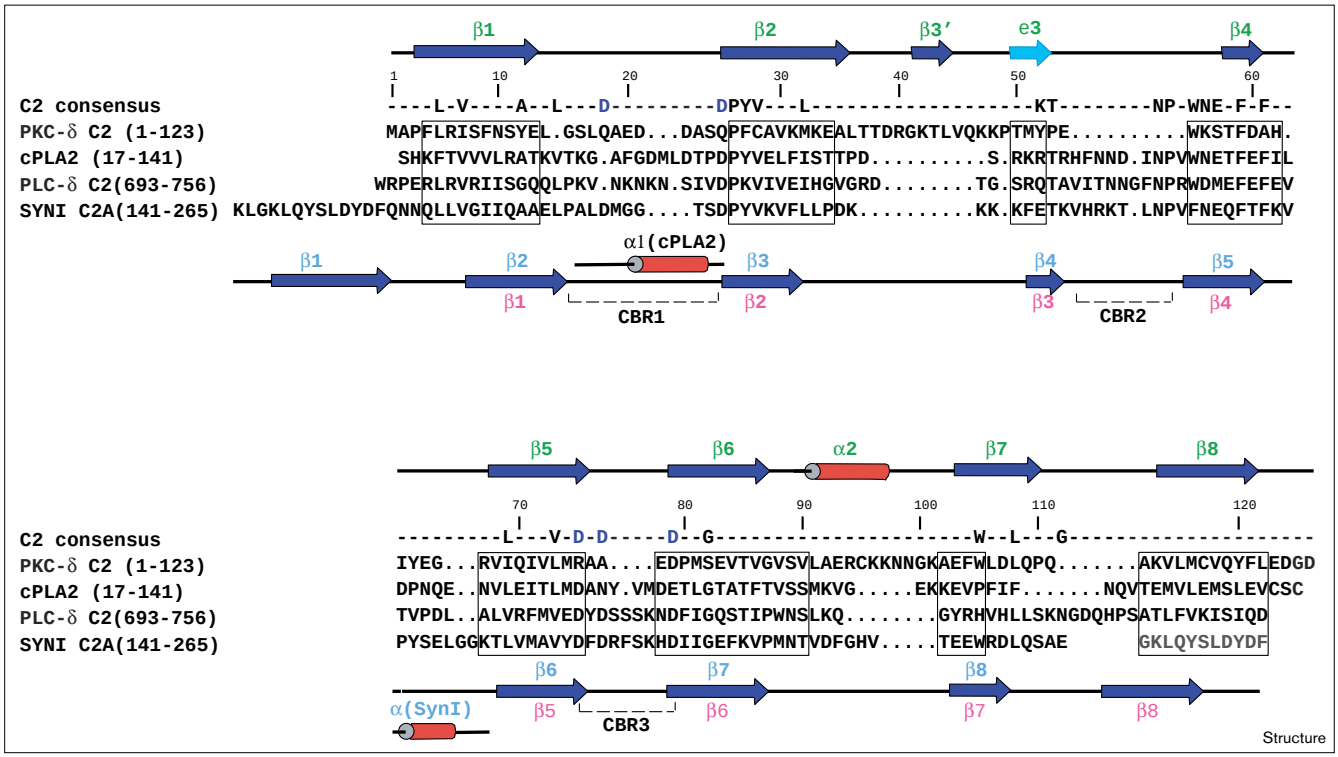

Structure-based sequence alignment of PKC-δ C2 with SynI, PLC-δ and cPLA2 C2 domains. Secondary structure (β strands, blue; extended strand, cyan; helices, red) was assigned by the program PROMOTIF [41]. The secondary structure elements of PKC-δ C2 (green), of SynI C2A (cyan), of PLC-δ C2 (magenta) and the Ca^{2+}-binding loops CBR1–3 are labelled. Boxed residues indicate structural equivalence based on alignment of the three domains by superposition and inspection in the program O [38].

Figure 5

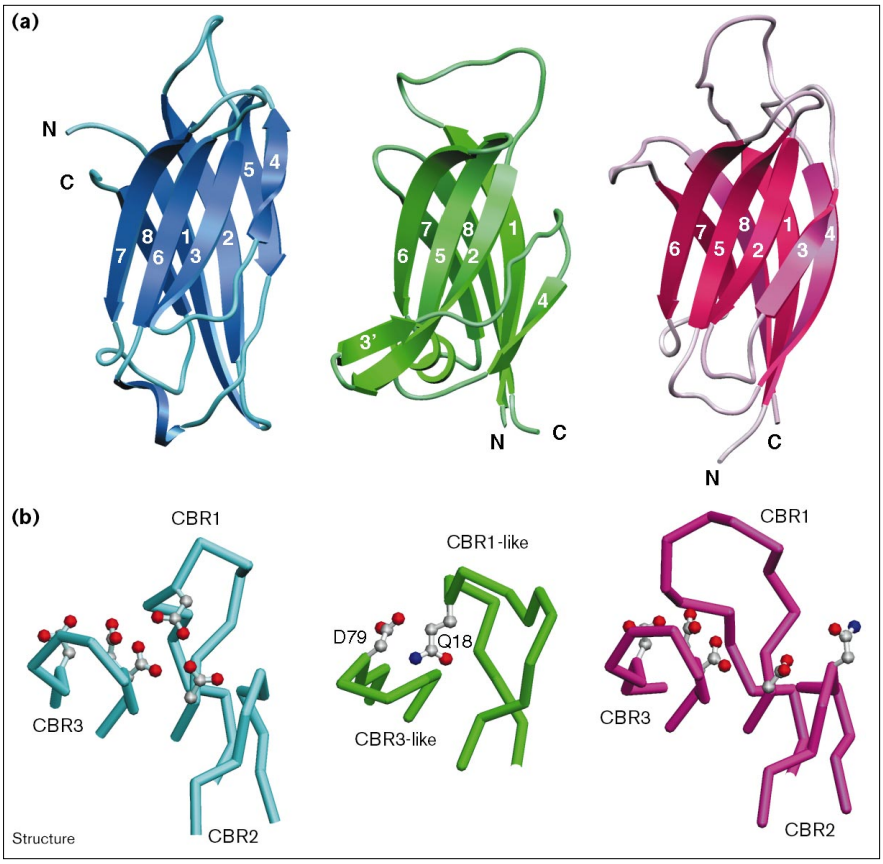

(a) A comparison of the structures for SynI C2A (cyan; PDB code 1rsy), PKC-δ C2 (green) and PLC-δ C2 (magenta; PDB code 1isd); β strands are numbered in white for comparison. (The figure was produced using the program SETOR [40].) **(b)** Comparison of the Ca^{2+}-binding loops of PLC-δ C2 (magenta) and SynI C2A (cyan) and the structurally equivalent loops from PKC-δ C2 (green). The three Ca^{2+}-binding loops of PLC-δ and SynI are labelled as CBR1, 2 and 3. Sidechains involved in Ca^{2+} coordination are shown for PLC-δ C2 and SynI, as are the equivalent sidechains of PKC-δ C2 domain. The corresponding PKC-δ C2 loops are described as CBR1-like and CBR3-like to indicate that although they are structurally equivalent, they do not bind Ca^{2+}. The CBR2-like loop of PKC-δ C2 is much shorter and is shifted by 13 Å relative to the other CBR2 loops (see text). It is therefore not represented in this figure.

alignment indicates that four core hydrophobic residues (Leu5, Pro28, Phe59 and Leu108) are absolutely conserved between the C2 structures, and several other core residues have only conservative substitutions (Figure 4). Three β bulges at Leu73, Arg75 and Ser82 occur at almost identical positions to those in SynI C2A [16] and PLC-δ [17], corresponding to residues Val228, Ile240 and Gly241 of SynI and Val704, Asp706 and Gly717 of PLC-δ. It is likely that these β bulges play important roles in maintaining the curvature and twisted nature of both β sheets.

Strands β1 and β2 are the longest strands in the structure and are connected by a 13-residue β1–β2 loop. This loop has relatively high temperature factors and the sidechains of Asp21 and Asp22, central to the loop, have been omitted from the refined model. Strand β2 continues away from the main body of the β sheet and hydrogen bonds to a strand we denote as β3′, for consistency with other C2 structures, forming a highly accessible and flexible β hairpin (residues Glu34 to Lys47). Within the hairpin, Gly41 has a positive ϕ torsion angle and residues Thr38 to Gly41 adopt different conformations between the two molecules within the asymmetric unit because of their involvement in a crystal lattice contact. Intermolecular contacts between the extremity of this loop and a neighbouring molecule are the only crystal contacts in the c-axis direction, explaining the variation of this axis dimension (between 115 Å and 122 Å) following cryocooling.

The hydrogen-bond pattern of the β2–β3′ hairpin is interrupted by a β bulge at Lys47. Residues Lys48 through to Pro53 form a short irregular strand with 'extended' conformation ϕ–ψ torsion angles, topologically equivalent to strand β3 of the PLC-δ C2 domain [17]. Despite the topological similarity, this strand, denoted as e3, makes only one pair of mainchain hydrogen bonds with strand β2 at Met51 and does not satisfy the criteria for a β strand defined by the program PROCHECK. [22]. A similar disruption of a β sheet is found in the distantly related structure of the C-terminal domain of diphtheria toxin (PDB accession number 1DDT) between strands 3 and 6. A hydrogen bond between the sidechains Gln46 and Thr50 (Nε2 Gln46 to Oγ1 Thr50 distance is 3.03 Å) also contributes to the e3-strand conformation.

Pro53, at the end of e3, is part of the invariant C2 motif Pro–X–Trp but is ~13 Å from the equivalent prolines in the PLC-δ and SynI C2A structures, which are located at

Figure 6

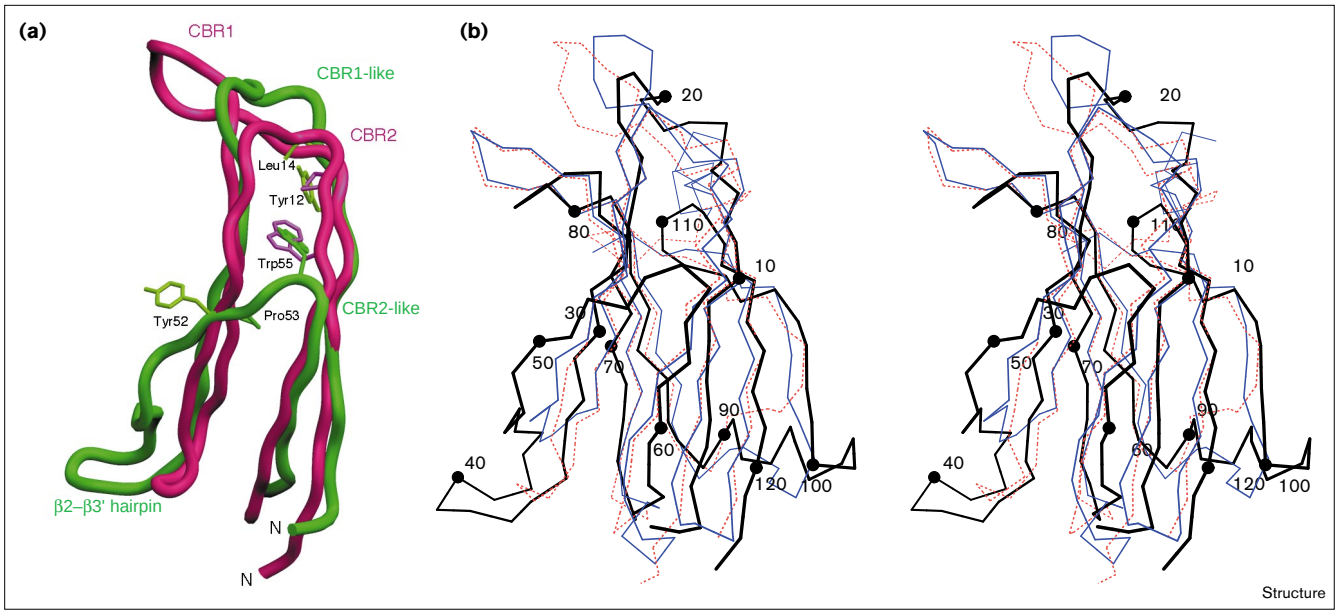

(a) Superposition of the C2 domains of PKC-δ (green) and PLC-δ (magenta) proximal to Trp55. (The figure was produced using the program SETOR [40].) **(b)** Superposition of Cα traces of PKC-δ C2 and the C2 domains of PLC-δ and SynI. The PKC-δ C2 is shown as a continuous black line with every tenth residue numbered, the SynI C2 as a thin blue line and the PLC-δ C2 as a dotted red line. (The figure was produced using the program MOLSCRIPT [42].)

the beginning of strand β4 in a quite different structural environment (Figures 4 and 6a). Similarly, the following turn (residues Glu54 to Ser57) positions Trp55 of the conserved C2 motif at (i+1) with its indole ring buried between the two β sheets. Although this sidechain superposes closely with Trp684 of PLC-δ within strand β4, both the rotamer and associated mainchain atoms are in quite different positions (Figure 6a). The good local sequence alignment of this region with other C2 sequences [15] is misleading when compared with a structural alignment (Figures 4 and 6b) and has implications for homology modelling of other C2 domains. Selective pressures may have forced the PKC-δ C2 structure to change, perhaps to evolve a specialised function, thereby trapping the sequence motif in a new structural environment.

The shortened length of strands e3 and β4 of PKC-δ C2 exposes to solvent sequences from adjacent strands β1 and β2. Compensatory changes to sequences in β1 fill the space created by this unusual C2 structure. For example, Tyr12 replaces the highly conserved buried alanine or glycine at this position in C2 domains, and its sidechain overlaps with Pro682 in strand β4 of PLC-δ (Figure 6a). Also, Leu14 of PKC-δ overlaps with the position of the mainchain atoms of Leu641 in PLC-δ. In contrast, no apparent sequence changes occupy the equivalent of the C-terminal end of PLC-δ strand β3, leaving Tyr52 of PKC-δ highly accessible (as will be discussed later).

The central strand β5 is connected via a type II′ β turn to strand β4 and forms multiple hydrogen bonds to both strands β2 and β6 in an antiparallel manner. Two β bulges at Leu73 (carboxyl end of strand β5) and Met81/Ser82 (amino end of strand β6) perturb the hydrogen-bond pattern between the strands with the consequence that the tips of these strands kink by almost 90° from the direction of the β sheet (Figure 3). A further structural element unique to PKC-δ C2 domain is the 8 residue α helix which replaces a long loop between strands β6 and β7, or their equivalents, in other C2 structures. It packs against the edge of both sheets and contributes several hydrophobic residues to the β-sandwich core, namely Val88, Leu91, Ala92 and Cys95. The helix, which we define as α2 for consistency with cPLA2 [18], ends with Gly100 which has a positive ϕ torsion angle and leads into strand β7. The highly twisted strand β7 connects to strand β8 by a short β turn which makes two mainchain hydrogen bonds (Gln109 to Glu83) across to strand β6 at precisely the same position as in PLC-δ. Following this turn, strand β8 continues through to Ala123 at the C terminus, adjacent to Ala1.

Comparison of PKC-δ C2 with the Ca^{2+}-binding regions of other C2-domain structures

The most striking difference between PKC-δ C2 and other C2 structures is found close to three loops clustered at one end of the C2 structure, equivalent to the functionally important Ca^{2+}-binding region of SynI and PLC-δ

(Figure 5b). Previous structural analyses have shown that C2 domains coordinate calcium ions through carboxylate groups from sidechain and mainchain atoms of two Ca^{2+}-binding loops, CBR1 (β1–β2) and CBR3 (β5–β6), with a shorter CBR2 (β3–β4) playing a supportive role [10,16–18]. The analogous three loops of PKC-δ C2 domain (referred to here as 'CBR-like') adopt quite different conformations and orientations, and lack all but one of the five conserved Ca^{2+}-coordinating sidechains present in PLC-δ C2 and SynI C2A (Figure 5b). The single conserved residue is Asp79 from the CBR3-like region (equivalent to Asp238 of SynI and Asp714 of PLC-δ; Figure 5b) whose sidechain forms a salt bridge with Arg75, thereby playing a structural role. The CBR1-like region has two aspartates, Asp21 and Asp22, within its sequence and therefore retains some acidic characteristics.

The CBR1-like loop projects away from the body of the structure but does not protrude to the extent of CBR1 from PLC-δ [17] or the helical CBR1 of cPLA2 [18]. Lacking supporting contacts from the CBR2 equivalent region, the CBR1-like loop is stabilised instead by a hydrophobic core comprising residues Tyr12, Leu14, Pro26 and Met81. Of these, Pro26 is highly conserved throughout the C2 superfamily and packs against the aromatic ring of Tyr12. Two additional structurally important residues influence the CBR1-like loop conformation — the buried Gln18 sidechain anchors the amino end of this loop through hydrogen bonds to mainchain amide (Gly15) and carbonyl (Met81) groups, and the sidechain of Gln111 hydrogen bonds to the Leu17 amide, providing further support to the amino end of the CBR1-like region.

The CBR3 loop of SynI, PLC-δ and cPLA2 has been implicated in membrane interaction and is oriented roughly perpendicular to the β sheet [16–18]. A similar conformation is found for the CBR3-like region of PKC-δ C2, though its shorter length (by four residues) and two negatively charged sidechains suggest that it may not be a principal determinant of lipid-bilayer interaction. The absence of Ca^{2+} binding to PKC-δ C2 prevents any potential neutralisation of this cluster of negative charges. A salt bridge between Arg75 and Asp79 is likely to organise the CBR3-like region conformation whilst the aliphatic portion of the Arg75 sidechain packs against the buried Met81 underneath the CBR1-like loop.

The position of the CBR2-like region is strikingly different from the position occupied by the CBR2 of other C2 structures. It adopts a reverse turn which is ~13 Å from CBR2 of PLC-δ (Cα of Trp55 in the CBR2-like region to Cα of Gly679 in PLC-δ CBR2). This shift is correlated with the extension of the β2–β3′ hairpin away from the tip of sheet B by 15 Å. The CBR2-like loop is therefore quite distant from the CBR1- or CBR3-like loops and lacks any of the basic sequences present in the CBR2 of many other C2 domains, as typified by the SynII C2B domain [23]. The observed differences between the CBR1, CBR2 and CBR3 loops of Ca^{2+}-binding C2 structures and the equivalent CBR-like loops in PKC-δ strongly suggest that the C2 domain of PKC-δ is unable to bind Ca^{2+}. Attempts to detect bound calcium or lanthanide ions following diffusion into crystals of PKC-δ C2 were not successful, consistent with the structural data.

Functionally important surfaces of novel PKC C2 domains involved in PKC translocation

The C2 domain of conventional PKC isotypes have been implicated in the translocation of PKC to specific subcellular compartments through promoting binding of Ca^{2+} and lipids such as phosphatidylserine [7]. The lipid-binding sequences and lipid preferences of these and other PKC C2 domains are, however, not well understood [7,9]. Models for lipid interaction have been proposed for the PLC-δ and cPLA2 Ca^{2+}-binding C2 domains whereby the hydrophobic CBR3 inserts into the membrane, whilst CBR1 and basic sequences within strand β3 interact with lipid head groups in the presence of Ca^{2+} [17,18]. For the novel PKC C2 domain, a different model for phospholipid binding is required as Ca^{2+} does not facilitate this interaction. The proper physiological activators of the novel PKCs remain to be established [12,24,25].

The distribution of basic and hydrophobic residues on the surface of PKC-δ C2 suggests that there are two potential lipid-binding surfaces. One of these comprises sequences from PKC-specific structural elements namely Lys33 and Lys42 within the β2–β3′ hairpin and Arg94 and Lys97 from helix α2 (Figure 7). This surface is rather flat and presents hydrophobic and polar sequences from the amino end of the CBR1-like loop and the β7–β8 loop towards a plane that is shared with the basic sequences (Figure 7). The surface is rotated roughly 90° with respect to other Ca^{2+}-dependent C2–lipid interaction models about an axis defined by the β2–β3′ hairpin and the β7–β8 loop (Figure 7). A second, smaller surface clusters Lys31 and Lys33 of strand β2 and residues Lys47 and Lys48 preceding strand e3, similar to the lipid-binding site of other C2 domains and close to Tyr52 [16–18]. The acidic residues Glu78 and Asp79 within the CBR3-like loop dominate this region and are unlikely to interact favourably with anionic phospholipid headgroups, however. Mutational analysis of these regions will clarify the precise role of individual sequences in lipid interaction.

A comparative analysis of different PKC isotypes identified PKC-δ as being tyrosine-phosphorylated in response to mitogen stimulation or phorbol-ester treatment [20,26]. A subsequent study identified a phosphorylation site at Tyr52 within the PKC-δ C2 domain, close to the CBR2-like loop and a different group of workers reported a site outside the C2 domain [27,28]. Consistent with the data of

Figure 7

Orthogonal views of the electrostatic surface of PKC-δ C2 calculated using the program GRASP [43]. Regions of positive charge are indicated in blue and regions of negative charge are in red. Specific sidechains and secondary structural elements are labelled for clarity. Sequences in helix α2, the β2–β3′ and β7–β8 hairpins and part of the CBR1-like region may interact with phospholipids.

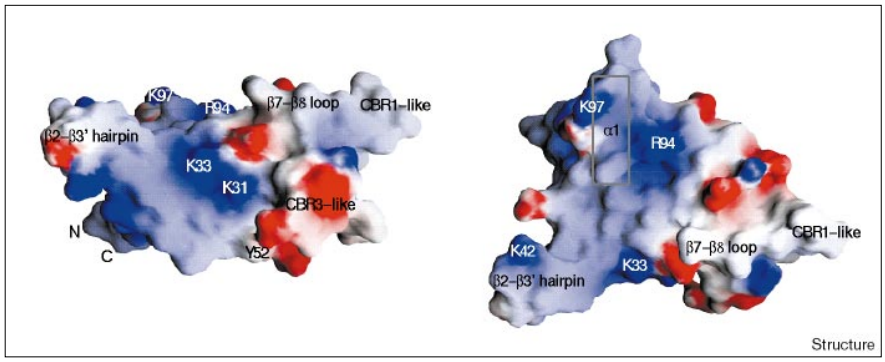

Szallasi *et al.* [27], Tyr52 is highly accessible within the sequence Met–Tyr52–Pro–Glu. This motif is similar to the preferred substrate sequence for the Fyn- and Lck-like Src-family tyrosine kinases implicated in targeting this site [29]. Sequences in this region of other novel PKCs either lack the tyrosine or, in the case of PKC-θ, the glutamate sidechain at the +2 position. It is possible that the distinct conformation of the CBR2-like region and the sequence context of Tyr52 are sufficient to explain why PKC-δ alone is tyrosine-phosphorylated *in vivo* in response to phorbol esters, whilst other PKC isotypes, either novel or conventional, are not [20]. Recent studies show that tyrosine-phosphorylated PKC-δ is localised in the cytosol whereas catalytically active PKC-δ is membrane-associated [26] suggesting that tyrosine modification may alter PKC-δ activity and membrane interaction.

PKC C2 domains also mediate PKC translocation through interaction with membrane-anchored PKC substrates [13] and binding proteins known collectively as RACKs [14]. For example, the PKC-δ C2 domain binds GAP43, a neuronal PKC substrate, *in vitro* and in transfected cells [13]. The molecular basis and physiological role for this interaction remain to be established. More detailed studies have investigated PKC C2 sequences responsible for RACK interaction [30,31]. Peptides derived from the CBR1-like region of PKC-ε, equivalent to residues 14–21 of PKC-δ, altered translocation of full-length PKC-ε in competition studies by blocking PKC binding to RACK [30]. This sequence is quite different from that of PKC-δ, however, and precedes an 11 residue insertion specific to PKC-ε and PKC-η. A separate study identified three peptides from PKC-βI that inhibited binding to the PKC-β RACK, RACK1 [31]. These peptides corresponded to sequences within strand β2 (PKC-β residues 186–198), the edge strands e3 (PKC-β residues 209–216) and β4 of PKC-δ (PKC-β residues 218–226) [28]. Consistent with this report, an anti-tumour agent and PKC inhibitor, dequalinium, prevents the formation of the PKC-β1–RACK1 complex by targeting Trp223 in strand β4 which corresponds to Trp55 of PKC-δ [32]. These data are of interest because RACKs bind only to activated PKC. The data imply that the RACK-binding sequences covering the edge of strands β3 and β4 of PKC-β1 and the CBR1-like loop of PKC-ε make interdomain contacts within inactive PKC and are exposed only following allosteric changes leading to PKC activation. The structural differences found in PKC-δ within these regions indicate that it is unlikely to bind to PKC-ε or PKC-β RACKs. This, taken together with PKC-specific tyrosine phosphorylation, suggests that the C2 structure may be responsible for the distinctive cellular localisation of PKC-δ [30].

PKC-δ C2 structure as a template for modelling homologous C2 domains and full-length novel PKCs

The novel PKC C2 domain closest in sequence to that of PKC-δ is PKC-θ (56% identity), and the conservation of core residues between these homologues suggests similar structures. In addition, the presence of a bulky sidechain at position 12 of strand β1 (tyrosine in PKC-δ and phenylalanine in PKC-θ) is highly indicative of a PKC-δ C2-like structure, as it replaces a buried alanine or glycine residue present in most C2 sequences [15]. As both PKC-ε and PKC-η C2 domains have alanine at this position, their structures may be closer to that of PLC-δ near the CBR2-like loop. It is therefore likely that PKC-δ and PKC-θ define a distinct subclass within the novel PKC isotypes. The low level of sequence similarity between the PKC-ε and PKC-η C2 domains and that of PKC-δ (19% and 16% identical respectively), as well as the presence of inserted or deleted sequences, particularly within regions such as the CBR1-like loop, indicate that further structural variations remain to be found amongst the novel PKC C2 domains. The extended sequences present in the CBR1-like loop of PKC-ε and PKC-η have been suggested to adopt a helical conformation similar to the cPLA2 CBR1, which is implicated in membrane interaction [18]. Both PKC-ε and PKC-η also differ from PKC-δ in the length of their CBR3-like loops and have shorter sequences connecting strands β6 and β7, suggesting the absence of helix α2.

Image reconstructions from electron micrographs of two-dimensional crystals of PKC-δ indicate a 'heart-shaped' structure [33]. It is tempting to position the C2 structure into one of the lobes of the heart and a pseudodimer of the C1 domain proposed by Srinivasan *et al.* [34] in the other, leaving the C3 and C4 domains to occupy the base. This aligns the lipid-binding surfaces of the C2 and C1 domains in the same orientation. The length of the connecting pseudosubstrate peptide from C2 to C1 indicates that these two modules are spatially close, as was proposed from functional data [12]. The intervening sequences between C1B and C3 (64 residues; see figure 1) are larger and will probably permit relative movement of domains during activation and translocation. The PKC–RACK binding site and PKC-δ tyrosine-phosphorylation site are likely to be buried, making interdomain contacts, and may become accessible only upon PKC activation. Differences between PKC-β and PKC-δ, evident from image reconstructions, hint at distinctive domain organisations as implied by sequence comparisons. Insights into the precise domain organisation of full length PKC-δ and the conformational changes necessary for proper activation must await a full crystallographic analysis.

Biological implications

The protein kinase C (PKC) family of lipid-dependent serine/threonine kinases are activated upon binding of multiple cofactors to conserved modules present within their N-terminal sequence. Diacylglycerol (DAG) binds to the C1 domain while Ca^{2+} and phospholipids such as phosphatidylserine bind to the C2 domain of conventional PKCs. C2 domains found within many other proteins also interact with phospholipids, thereby assisting protein translocation to an appropriate lipid environment.

We report here the structure of a C2 domain from PKC-δ, a member of the novel class of PKCs which are Ca^{2+}-independent but require both DAG and phosphatidylserine for activation. The structure indicates that the molecular basis for this Ca^{2+}-independence results from major structural differences within the C2 domain compared to other C2 domains. Three spatially close loops of PKC-δ C2 adopt radically different conformations from the equivalent Ca^{2+}-binding loops of other C2 structures and lack their Ca^{2+}-coordinating sequences. One of these loops contains a tyrosine-phosphorylation site, explaining why PKC-δ is tyrosine-phosphorylated *in vivo* in response to phorbol esters, in contrast to other PKC isotypes.

We propose that basic sequences within two PKC-δ C2-specific secondary structures may define a lipid-interaction site distinct from that of the conventional PKC C2 domain and may account for their different affinities for lipid *in vitro*. A highly conserved C2 sequence motif adopts a different conformation from that of other C2 domains, illustrating the need for representative examples of structural variants within a protein superfamily in order to build accurate homology models. On the basis of our structure, the C2 domains of PKC-δ and PKC-θ should be separated into a different subclass from PKC-ε and PKC-η, whose CBR2-like loop is likely to be closer to that of PLC-δ. The unique features of the PKC-δ C2 structure may underlie the distinctive cellular localisation of activated PKC-δ.

Materials and methods

Crystallisation and data collection

Preparation, purification and crystallisation of the recombinant native and selenomethionine substituted PKC-δ C2 domain has been described previously [21]. Briefly, recombinant C2 domain was produced using a pET-14b expression vector which placed a polyhistidine tag at the N terminus of the construct. Crystals of untagged PKC-δ C2 domain were grown from 20% PEG 4000, 0.1 M sodium citrate, 0.2 M ammonium acetate, pH 5.6, and were stable at room temperature. The crystals grew as thin elongated plates and diffracted to 2.2 Å using a synchrotron source. Native and derivative X-ray data were recorded from single crystals at room temperature. Although data could be measured from cryo-cooled crystals, severe non-isomorphism from the irreproducible variation of the unit cell parameters hampered structure determination.

For derivative searches, crystals were equilibrated against solutions of the metal salts in 27.5% PEG 4000, 0.1 M Tris/Acetate, 0.2 M ammonium acetate, pH 6.0. Good quality derivatives were obtained from 1 mM phenyl mercury chloride (PheHgCl) after 30 h soaking at 4°C and from 0.1 mM ethyl mercury thiosalicylate (EMTS) soaked at 4°C for 18 h. All diffraction data, except the EMTS dataset, were collected on a MAR image plate in the Daresbury synchrotron source. The EMTS dataset was collected on an R-AXIS image plate mounted on a Rigaku RU-300 rotating anode X-ray generator operated at 50 kV and 90 mA. Integrated intensities were obtained with DENZO software from the HKL suite [35] and data reduction was performed with the programs SCALEPACK [35] and AGROVATA from the CCP4 suite [36].

Phasing and model building

The structure of the PKC-δ C2 domain was determined using phase information from two mercury derivatives and a selenomethionine dataset (Table 1). Difference Patterson maps for the PheHgCl and EMTS derivative were solved by inspection and the resulting sites were refined using the program SHARP [37]. The initial maps from SHARP were improved by solvent flattening, as implemented in the program SOLOMON. A molecular boundary for each of the two molecules in the asymmetric unit was apparent from the density modified maps. An operator describing the relative positions of the two molecules in the asymmetric unit was derived by inspection of this map and refined using the program IMP [38]. A mask was created from a partial model of molecule 1. The phases obtained from the program DM [36] were then used to crossphase a difference Fourier map using data from a selenomethionine derivative and, five selenomethionine sites on each molecule (molecules 1 and 2), related by the non-crystallographic symmetry (ncs) operator, were subsequently identified (Figure 2). A further cycle of SHARP including the two mercury derivatives and the selenium derivative, followed by solvent flattening and ncs averaging in DM, provided a map in which we were able to build most of both molecules, except for the loop connecting strands β1 and β2. Model building was performed using the program O [38].

Refinement

An initial model was built into the 2.5 Å averaged maps and was the starting point for refinement. Restraints were set by the program PROTIN before proceeding with maximum-likelihood refinement as implemented by the program REFMAC, using stringent ncs restraints [36]. Density for the loop connecting strands β1 and β2 (residues 18–24) became apparent only after several cycles of refinement applying weak ncs

Table 1

Data collection and phasing statistics for PKC-δ C2 domain.

	Native	PheHgCl	EMTS	Selenomethionine
Wavelength (Å)	0.87	0.87	1.54	0.98
Resolution (Å)	2.3	3.0	3.2	2.8
Completeness (%)	96.0	87.8	94.7	97.1
R_{sym}*	7.1	6.4	8.6	7.9
Total reflections	36,783	18,821	15,950	35,815
Unique reflections	13,223	5570	4961	7565
Unique Bijvoet pairs	–	3993	3638	5926
R_{iso}†	–	0.44	0.20	0.16
Number of sites	–	2	3	5
Phasing power‡ centrics	–	1.3	1.1	1.4
Phasing power‡ acentrics-iso	–	1.5	1.4	1.6
Phasing power‡ acentrics-ano	–	3.6	1.2	2.1

All datasets were recorded from a single crystal. *R_{sym} is defined as $\Sigma|Io-\langle I\rangle| / Io$, where Io values are observed intensities and $\langle I\rangle$ values are average intensities for redundant measurements. †R_{iso} is the mean fractional difference calculated between native and derivative structure-factor amplitudes. ‡The phasing power is defined as rms ($|F_H| / E$), where E is the residual lack of closure error.

restraints and model building. The program X-PLOR was used during the final rounds of refinement including a bulk solvent correction and overall anisotropic B factor [39]. The stereochemical quality of the model as assessed by PROCHECK [22] was good, with an rmsd of 0.01 Å from ideal bond lengths and 1.4° for bond angles. The final model includes 1,926 non-hydrogen protein atoms and 74 water molecules, with an R factor of 19.5% and R free of 24.5% for all data between 20 Å and 2.2 Å. Electron density is poor for residues 18–22 of both molecules and sidechains have been omitted for Glu20, Asp21 and Asp22 of molecule 1, and Asp21 and Gln25 of molecule 2. Residues 17 of molecule 1 and residues 22 and 56 of molecule 2 are outliers on the Ramachandran plot.

Accession numbers

Coordinates have been deposited in the Brookhaven Protein Data Bank under accession number 1BDY.

Acknowledgements

HP was supported by a Marie Curie TMR from the European Commission (ERBFMBICT96-1786). We thank all members of the Structural Biology Laboratory for helpful discussions and encouragement. We also gratefully acknowledge the use of SRS facilities at Daresbury.

References

1. Dekker, L.V., Palmer, R.H. & Parker, P.J. (1995). The protein-kinase-C and protein-kinase-C related gene families. *Curr. Opin. Struct. Biol.* **5**, 396-402.
2. Newton, A.C. (1995). Protein kinase C: structure, function, and regulation. *J. Biol. Chem.* **270**, 28495-28498.
3. Hanks, S.K., Quinn, A.M. & Hunter, T. (1988). The protein kinase family: conserved features and deduced phylogeny of the catalytic domains. *Science* **241**, 42-52.
4. Orr, J.W. & Newton, A.C. (1994). Requirement for negative charge on "activation loop" of protein kinase C. *J. Biol. Chem.* **269**, 27715-27718.
5. Hurley, J.H., Newton, A.C., Parker, P.J., Blumberg, P.M. & Nishizuka, Y. (1997). Taxonomy and function of C1 protein kinase C homology domains. *Protein Sci.* **6**, 477-480.
6. Ponting, C.P. & Parker, P.J. (1996). Extending the C2 domain family: C2s in PKCs δ, ε, η, θ, phospholipases, GAPs and perforin. *Protein Sci.* **5**, 162-166.
7. Newton, A.C. (1997). Regulation of protein kinase C. *Curr. Opin. Cell Biol.* **9**, 161-167.
8. Zhang, G., Kazanietz, M.G., Blumberg, P.M. & Hurley, J.H. (1995). Crystal structure of the Cys2 activator-binding domain of protein kinase Cδ in complex with phorbol ester. *Cell* **81**, 917-924.
9. Edwards, A.S. & Newton, A.C. (1997). Regulation of protein kinase C βII by its C2 domain. *Biochemistry* **36**, 15615-15623.
10. Shao, X., Davletov, B.A., Sutton, B., Sudhof, T.C. & Rizo, J. (1996). Bipartite Ca^{2+}-binding motif in C2 domains of synaptotagmin and protein kinase C. *Science* **273**, 248-251.
11. Newton, A.C. (1996). Protein-kinase-C – ports of anchor in the cell. *Curr. Biol.* **6**, 806-809.
12. Pepio, A.M. & Sossin, W.S. (1998). The C2 domain of the calcium-independent protein kinase C aplII inhibits phorbol ester binding to the C1 domain in a phosphatidic acid-sensitive manner. *Biochemistry* **37**, 1256-1263.
13. Dekker, L.V. & Parker, P.J. (1997). Regulated binding of the protein kinase C substrate GAP-43 to the V0/C2 region of protein kinase C-δ. *J. Biol. Chem.* **272**, 12747-12753.
14. Mochly-Rosen, D. (1995). Localization of protein-kinases by anchoring proteins – a theme in signal-transduction. *Science* **268**, 247-251.
15. Nalefski, E.A. & Falke, J.J. (1996). The C2 domain calcium-binding motif: structural and functional diversity. *Protein Sci.* **5**, 2375-2390.
16. Sutton, R.B., Davletov, B.A., Berghuis, A.M., Sudhof, T.C. & Sprang, S.R. (1995). Structure of the first C2 domain of synaptotagmin I: a novel Ca^{2+}/phospholipid-binding fold. *Cell* **80**, 929-938.
17. Essen, L-O., Perisic, O., Cheung, R., Katan, M. & Williams, R.L. (1997). Crystal structure of a mammalian phosphoinositide-specific phospholipase Cδ. *Nature* **380**, 595-602.
18. Perisic, O., Fong, S., Lynch, D.E., Bycroft, M. & Williams, R.L. (1998). Crystal structure of a calcium-phospholipid binding domain from cytosolic phospholipase A2. *J. Biol. Chem.* **273**, 1596-1604.
19. Essen, L-O., Perisic, O., Lynch, D.E., Katan, M. & Williams, R.L. (1997). A ternary metal binding site in the C2 domain of phosphoinositide-specific phospholipase C-δ1. *Biochemistry* **36**, 2753-2762.
20. Li, W., Mischak, H., Yu, J., Wang, L., Mushinski, J.F., Heidaran, M.A. & Pierce, J.H. (1994). Tyrosine phosphorylation of protein kinase C-δ in response to its activation. *J. Biol. Chem.* **269**, 2349-2352.
21. Pappa, H.S., Dekker, L.V., Parker, P.J. & McDonald, N.Q. (1998). Preliminary X-ray analysis of a C2-like domain from protein kinase C-δ. *Acta Cryst. D*, in press.
22. Laskowski, R.A., MacArthur, M.W., Moss, D.S. & Thornton, J.M. (1993). PROCHECK: a program to check the stereochemical quality of protein structures. *J. Appl. Cryst.* **26**, 283-291.
23. Fukuda, M., Kojima, T., Aruga, J., Niinobe, M. & Mikoshiba, K. (1995). Functional diversity of C2 domains of synaptotagmin family. *J. Biol. Chem.* **270**, 26523-26527.
24. Medkova, M. & Cho, W. (1998). Differential membrane-binding and activation mechanisms of protein kinase C-α and -ε. *Biochemistry* **37**, 4892-4900.
25. Toker, A., *et al.*, & Cantley, L.C. (1994). Activation of protein kinase C family members by the novel polyphosphoinositides PtdIns-3,4-P2 and PtdIns-3,4,5-P3. *J. Biol. Chem.* **269**, 32358-32367.
26. Shanmugam, M., *et al.*, & Hunzicker-Dunn, M. (1998). Association of protein kinase Cδ and active Src in PMA-treated MCF-7 human breast cancer cells. *Oncogene* **16**, 1649-1654.
27. Szallasi, Z., *et al.*, & Blumberg, P.M. (1995). Development of a rapid approach to identification of tyrosine phosphorylation sites: application to PKC-δ phosphorylated upon activation of the high affinity receptor for IgE in rat basophilic leukemia cells. *Biochem. Biophys. Res. Commun.* **214**, 888-894.
28. Li, W., *et al.*, & Pierce, J.H. (1996). Identification of Tyrosine 187 as a protein kinase C-δ phosphorylation site. *J. Biol. Chem.* **271**, 26404-26409.
29. Songyang, Z., *et al.*, & Cantley, L.C. (1995). Catalytic specificity of protein tyrosine kinases is critical for selective signalling. *Nature* **373**, 536-539.
30. Johnson, J.A., Gray, M.O., Chen, C-H. & Mochly-Rosen, D. (1996). A protein kinase C translocation inhibitor as an isozyme-selective antagonist of cardiac function. *J. Biol. Chem.* **271**, 24962-24966.

31. Ron, D., Luo, J. & Mochly-Rosen, D. (1995) C2 region-derived peptides inhibit translocation and function of β protein kinase C *in vivo*. *J. Biol. Chem.* **270**, 24180-24187.
32. Rotenburg, S.A. & Sun, X. (1998). Photoinduced inactivation of protein kinase C by dequalinium identifies the RACK-1-binding domain as a recognition site. *J. Biol. Chem.* **273**, 2390-2395.
33. Owens, J.M., Kretsinger, R.H., Sando, J.J. & Chertihin, O.I. (1998). Two-dimensional crystals of protein kinase C. *J. Struct. Biol.* **121**, 61-67.
34. Srinivasan, N., Bax, B., Blundell, T.L. & Parker, P.J. (1996). Structural aspects of the functional modules in human protein kinase Cα deduced from comparative analyses. *Proteins* **26**, 217-235.
35. Gewirth, D. (1994). The HKL manual: an oscillation data processing suite for macromolecular crystallography. Department of Molecular Biophysics and Biochemistry, Yale University, New Haven, CT, USA.
36. Collaborative Computational Project Number 4. (1994). The CCP4 suite: programs for protein crystallography. *Acta Cryst. D* **50**, 760-763.
37. La Fortelle, E. & Bricogne, G. (1997). Maximum-likelihood heavy atom parameter refinement for multiple isomorphous replacement and multiwavelength anomalous diffraction methods. *Methods Enzymol.* **276**, 472-494.
38. Jones, T.A., Zou, J.Y., Cowan, S.W. & Kjeldgaard, M. (1991). Improved methods for building protein models in electron density maps and the location of errors in these models. *Acta Cryst. A* **47**, 110-119.
39. Brünger, A.T. (1992). X-PLOR *Version 3.1: A System for X-ray Crystallography and NMR*. Department of Molecular Biophysics, Yale University, New Haven, CT, USA.
40. Evans, S.V. (1993). SETOR hardware lighted 3-dimensional solid model representations of macromolecules. *J. Mol. Graphics* **11**, 134-138.
41. Hutchinson, E.G. & Thornton, J.M. (1996). PROMOTIF—a program to identify and analyze structural motifs in proteins. *Protein Sci.* **5**, 212-220.
42. Kraulis, P.J. (1991). MOLSCRIPT: a program to produce both detailed and schematic plots of protein structures. *J. Appl. Cryst.* **24**, 946-950.
43. Nicholls, A., Sharp, K. & Honig, B. (1991). Protein folding and association: insights from the interfacial and thermodynamic properties of hydrocarbons. *Proteins* **11**, 281-296.